Astronomy & Astrophysics manuscript no. 4079 February 5, 2008
(DOI: will be inserted by hand later)

Extrasolar planets and brown dwarfs around A-F type stars ⋆

IV. A candidate brown dwarf around the A9V pulsating star HD 180777.

F. Galland[1,2], A.-M. Lagrange[1], S. Udry[2], J.-L. Beuzit[1], F. Pepe[2], and M. Mayor[2]

[1] Laboratoire d'Astrophysique de l'Observatoire de Grenoble, Université Joseph Fourier, BP 53, 38041 Grenoble, France
[2] Observatoire de Genève, 51 Ch. des Maillettes, 1290 Sauverny, Switzerland

Received August 22, 2005 / Accepted February 06, 2006

Abstract.
We present here the detection of a brown dwarf orbiting the A9V star HD 180777. The radial velocity measurements, obtained with the ELODIE echelle spectrograph at the Haute-Provence Observatory, show a main variation with a period of 28.4 days. Assuming a primary mass of 1.7 $M_{\odot}$, the best Keplerian fit to the data leads to a minimum mass of 25 M_{Jup} for the companion (the true mass could be significantly higher). We also show that, after substraction of the Keplerian solution from the radial velocity measurements, the residual radial velocities are related to phenomena intrinsic to the star, namely pulsations with typical periods of γ Dor stars. These results show that in some cases, it is possible to disentangle radial velocity variations due to a low mass companion from variations intrinsic to the observed star.

Key words. techniques: radial velocities - stars: early-type - stars: brown dwarfs - stars: variable - stars: individual: HD 180777

1. Introduction

Radial velocity surveys have lead to the detection of more than 160 planets during the past decade [1]. We are performing a radial velocity survey dedicated to the search for extrasolar planets and brown dwarfs around a volume-limited sample of more massive stars than currently done, namely A-F main-sequence stars (i) with the ELODIE fiber-fed echelle spectrograph (Baranne et al. 1996) mounted on the 1.93-m telescope at the Observatoire de Haute-Provence (CNRS, France) in the northern hemisphere, and (ii) with the HARPS spectrograph (Pepe et al. 2002) installed on the 3.6-m ESO telescope at La Silla Observatory (ESO, Chile) in the southern hemisphere. Finding planets and brown dwarfs around massive stars is important, as this will allow us to test planetary formation and evolution processes around a wider variety of objects.

As A-F main-sequence stars exhibit a small number of stellar lines, usually broadened and blended by stellar rotation, we developed a new radial velocity method that is described in Galland et al., 2005a (Paper I), together with the detection limits we achieved and the estimates of the minimum detectable masses. The first results of the survey are (i) discovering with ELODIE a planet around an F6V star (Galland et al., 2005b, Paper II), and (ii) finding the limits to the presence of an inner giant planet around β Pictoris, with HARPS and CORALIE (Galland et al., 2006a, Paper III); in this last case, the observed radial velocity variations are attributed to δ Scuti type pulsations.

We present here the detection of a brown dwarf around one of the objects surveyed with ELODIE, HD 180777. Section 2 provides the stellar properties of this star. Section 3 explains the measurement of the radial velocities, and the Keplerian solution associated to the main radial velocity variations is derived in Sect. 4. In Sect. 5, we rule out other possible origins of these main radial velocity variations. The large radial velocity residuals around the orbital solution are interpreted in terms of pulsations in Sect. 6.

2. Stellar properties

HD 180777 (HIP 94083, HR 7312) is located at 27.3 pc from the Sun (ESA 1997). Its projected rotational velocity, calculated using auto-correlation, is $v \sin i = 50\,\mathrm{km\,s^{-1}}$; if the true rotational velocity of this star meets the mean rotational velocity of A9V type stars, namely $125\,\mathrm{km\,s^{-1}}$ (Gray 2005), the value of $\sin i$ would be 0.4. The effective temperature $T_{eff} = 7250\,\mathrm{K}$ and the surface gravity $\log g = 4.34$ are taken from King et al. (2003). The stellar properties are summarized in Table 1. Note that the MK spectral type of HD 180777 varies from A9V to F2V depending on the au-

Send offprint requests to: F. Galland,
e-mail: Franck.Galland@obs.ujf-grenoble.fr

⋆ Based on observations made with the ELODIE spectrograph at the Observatoire de Haute-Provence (CNRS, France).

[1] A comprehensive list of known exoplanets is available at http://www.obspm.fr/encycl/cat1.html

Table 1. HD 180777 stellar properties. Photometric and astrometric data are extracted from the HIPPARCOS catalogue (ESA 1997). Spectroscopic data are from King et al. (2003).

Parameter		HD 180777
Spectral Type		A9V
$v \sin i$	[km s^{-1}]	50
V		5.11
B-V		0.308
π	[mas]	36.6
Distance	[pc]	27.3
M_V		2.93
T_{eff}	[K]	7250
$\log g$		4.34
M_1	[M$_\odot$]	1.7

thors; yet, the spectral type A9V is more frequent (see e.g. the HIPPARCOS catalogue, ESA 1997, or the Bright Star Catalogue, Hoffleit et al. 1991). Given this spectral type, we deduce a stellar mass of 1.7±0.1 M$_\odot$.

HD 180777 belongs to the range of B-V where the instability strip intersects with the main sequence. This region contains the pulsating δ Scuti (Handler et al. 2002, Breger et al. 2000) and γ Dor stars (Mathias et al. 2004), with respective stellar mass ranges of [1.5, 2.2] M$_\odot$ and [1.2, 1.9] M$_\odot$. With a mass of ≈ 1.7 M$_\odot$, HD 180777 could then belong to one or the other class of pulsating stars. We show in Sect. 6 that HD 180777 actually undergoes pulsations with frequencies associated to the γ Dor stars.

3. Radial velocity measurements

By July 2005, 45 spectra of HD 180777 were acquired with ELODIE, over 690 days. The wavelength range of the spectra is 3850-6800 Å. Six spectra obtained under bad weather conditions (with an absorption larger than 2 mag) were discarded. The typical exposure time was 15 min, leading to an S/N equal to ∼ 190. The exposures were performed without the simultaneous-thorium mode usually used to follow and correct for the local astroclimatic drift of the instrument; a wavelengh calibration was performed each hour, however, which is largely sufficient to correct for the drift in the case of ELODIE and when the radial-velocity photon-noise uncertainties are larger than a few dozens m s^{-1}. In this way, the spectra obtained are not polluted by the stronger Thorium lines spread on the CCD, a mandatory requirement for our method with A-F spectral type stars (see Paper I).

For each spectrum, we selected 34 spectral orders with high contrast, covering a wavelength range of 4100-5700 Å and avoiding orders containing calcium and hydrogen lines or contaminated by telluric absorption lines. Assuming that the spectra are translated (stretching in the wavelength space) from one to the other, the radial velocities were measured using the method described in Chelli (2000) and Paper I. They are displayed in Fig. 1 (top). The uncertainty of 64 m s^{-1} on average is consistent with the value of 70 m s^{-1} obtained from simulations

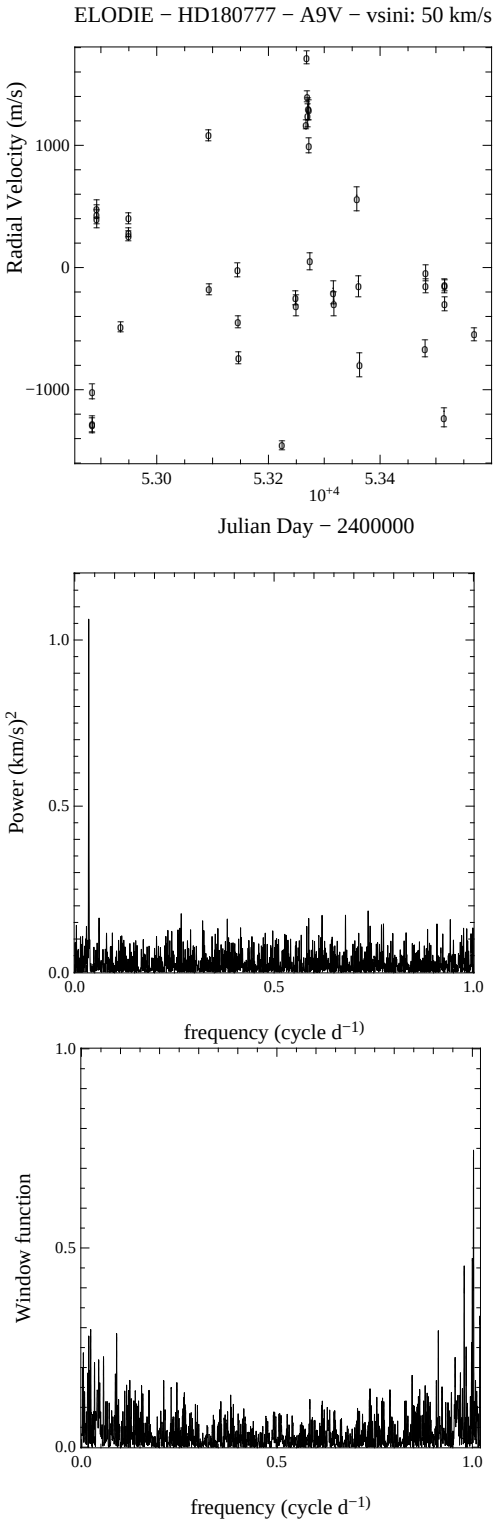

Fig. 1. Radial velocities of HD 180777 obtained with ELODIE (top), the associated periodogram (center) and the window function (bottom).

in Paper I by applying the relation between the radial velocity uncertainties and $v \sin i$ to HD 180777, with S/N values equal to 190. The observed radial velocities are found to be variable with a much larger amplitude than the uncertainties.

The periodogram of the radial velocities is displayed in Fig. 1 (center). We used the CLEAN algorithm (Roberts et al 1987) in order to remove the aliases linked with the temporal sampling of the data (this algorithm iteratively deconvolves the window function from the initial "dirty" spectrum). We used only one iteration here, with a gain loop value of one. A clear peak appears at a period of 28.4 days. It is not a sampling effect, given the window function (Fig. 1, bottom). Figure 2 shows the radial velocities phased with this period. It is consistent with this periodicity in the radial velocity variations. In addition, we calculated the false-alarm probability of this signal. To do so, we performed a Fisher randomization test (Linnell Nemec & Nemec 1985): the radial velocities are shuffled randomly with the same time-series as observations, then the periodogram is calculated; this is repeated many times (50 000 here), and the number of periodograms containing a power higher than the one for the 28.4 days signal in the measured radial velocities is stored. The false-alarm probability found this way is lower than 2.10^{-5}, confirming the significance of this 28.4 days signal.

4. A brown dwarf around HD 180777

4.1. Main variation: orbital parameters

We fit the radial velocities with a Keplerian solution (Fig. 2). The orbital parameters derived from the best solution are given in Table 2. The amplitude is 1.2 km s^{-1}, which is consistent with the value of the peak in the previous periodogram. The orbital period is 28.4 days, and the eccentricity is 0.2. Assuming a primary mass of 1.7 $M_\odot$, the companion mass falls in the brown-dwarf domain, with a minimum mass of 25 M_{Jup}. Note that a value of 0.4 for $\sin i$ (see Sect. 2) would result in a true mass value of 62 M_{Jup}; we even cannot completely exclude the case of a low mass M dwarf. The separation between this candidate brown dwarf and the star is 0.2 AU. The dispersion of the residuals is 394 m s^{-1}. They are much larger than uncertainties (also clearly seen on the individual residuals, Fig. 2), suggesting another source of radial velocity variations. This source should not be a companion since there is no satisfactory Keplerian fit to these residuals considering the case of only one companion (in addition to the above brown dwarf).

Table 2. ELODIE best orbital solution for HD 180777.

Parameter		HD 180777
P	[days]	28.44± 0.01
T	[JD-2400000]	53244.3± 0.3
e		0.20 ± 0.01
γ	[km s^{-1}]	0.11± 0.01
ω	[deg]	56 ± 4
K	[km s^{-1}]	1.20 ± 0.02
N_{meas}		39
$\sigma(O-C)$	[km s^{-1}]	0.394
$a_1 \sin i$	[10^{-3} AU]	3.1
f(m)	[$10^{-6} M_\odot$]	4.7
M_1	[$M_\odot$]	1.7
$m_2 \sin i$	[M_{Jup}]	25
a	[AU]	0.22

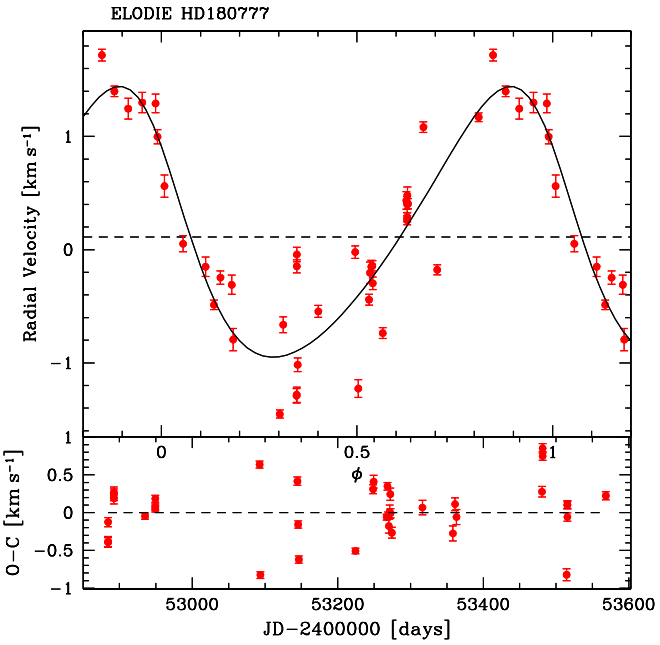

Fig. 2. Top: ELODIE radial velocities and orbital solutions for HD 180777. Bottom: Residuals to the fitted orbital solution.

4.2. Checking the translation of the spectra

We check here that the above periodic signal is only due to a periodic translation of the spectra, without simultaneous change in the shape of the lines that would correspond to variations that are intrinsic to the star. To do so, we compute the cross-correlation function of each spectrum with a binary mask. These correlation functions represent the mean line profile of each spectrum, and they are displayed in Fig. 3 (top, left). Note that this is a standard way to measure the radial velocities for solar-type stars. The correlation functions show a dispersion from one to the other, potentialy due in part to a translation, visible in particular in the zones of large slope. The dispersion of the positions of Gaussian fits made considering only these zones is 870 m s^{-1}.

In order to detect periodic variations in the lines of the spectra, we calculated the temporal periodogram corresponding to each point of the cross-correlation functions. We then summed all these periodograms, so as to enhance the variations occuring along all the cross-correlation functions. This summed periodogram is displayed in Fig. 3 (top, right). A clear peak appears at a frequency corresponding to a period of 28.4 days. The radial velocities found considering the center of the Gaussian fits are consistent with the ones measured in Sect. 3, given the uncertainties.

We then translated the cross-correlation functions to correct them from the orbital solution found in Sect 4.1. The results are displayed in Fig. 3 (bottom, left). The dispersion of the positions of Gaussian fitted only to the zones of large slope is now 410 m s^{-1}, half the value found previously. It is also consis-

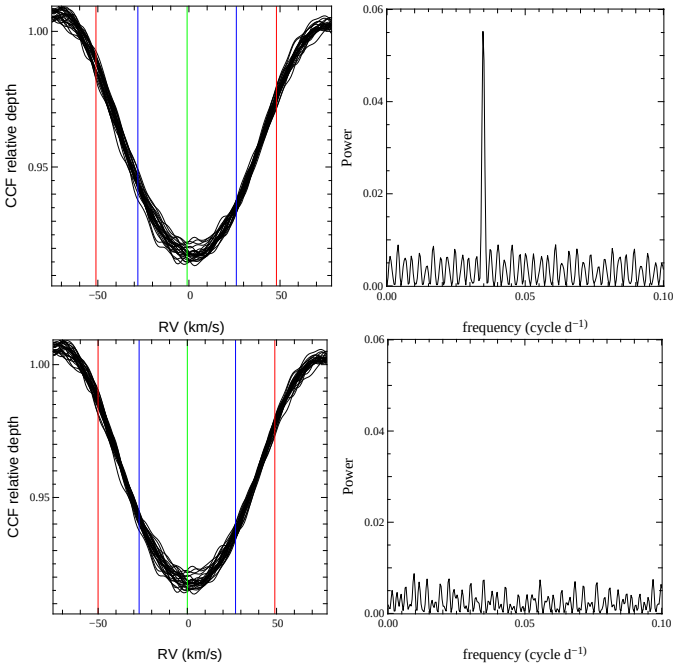

Fig. 3. Left: cross-correlation functions of HD 180777, before (top) and after (bottom) correction from the Keplerian motion. Right: their corresponding summed periodograms (see text), with the same scale in the two cases.

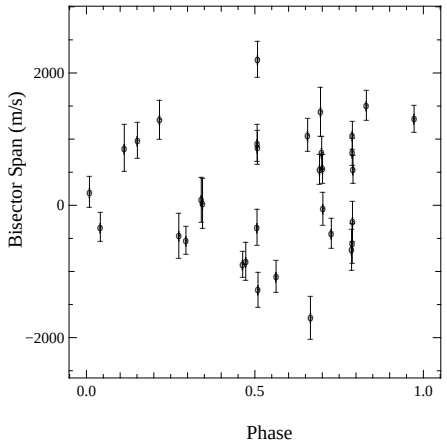

Fig. 4. Span of the cross-correlation functions phased with a period of 28.44 days: no periodic variation with this period.

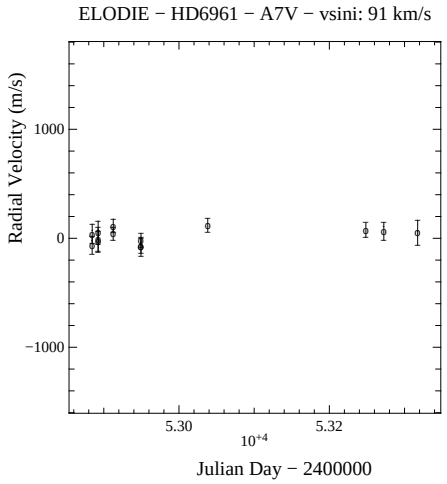

Fig. 5. ELODIE radial velocity data for HD 6961, a star constant in radial velocity (dispersion of 63 m s^{-1}), similar and close to HD 180777. The vertical scale is identical to the one in Fig. 1.

tent with the dispersion of the radial-velocity residuals around the Keplerian solution. This is a first check of the reality of the translation of the spectra from one to the others. Moreover, the summed periodogram, displayed in Fig. 3 (bottom, right), does not show any peak at the frequency corresponding to a period of 28.4 days. This confirms that the cross-correlation functions were effectively translated from one to the others, and that the fit of the radial velocities is accurate. Note that a correcting translation of the cross-correlation functions made at a wrong period and/or a wrong amplitude would produce or enhance a peak at the corresponding frequency in the summed periodogram, instead of removing it. In the same way, if there was no initial translation in the spectra but only changes in the shapes of the lines, the peak in the periodogram would not disappear after corrected translation of the cross-correlation functions.

We finally check that this periodic translation of the spectra is not accompanied by simultaneous changes in the shape of the lines with the same period of 28.44 days. Figure 4 shows the span (or inverse slope) of the bisectors of the cross-correlation functions, phased with this period. They are significantly variable, indicating changes in the shape of the lines (see Sect. 6), but there is no periodic variation in the spans with a period of 28.44 days. Hence, the 28-d signal corresponds only to a shift of the spectra, and not to a change in the line shape. The existence of a brown dwarf is the best explanation for this signal.

5. Ruling out other origins of the main 28-d variations

5.1. A single star

We checked that HD 180777 is not a blended double-lined spectroscopic binary. In such a case, the FWHM of the cross-correlation functions is expected to be linked with their depth (anti-correlation). No such correlation is observed for HD 180777.

5.2. A similar star constant in radial velocity

HD 180777, with a declination of +76 degrees, is located far from the ecliptic plane, i.e. always far from the Moon. Moreover, the spectral type of the Sun, whose light is reflected

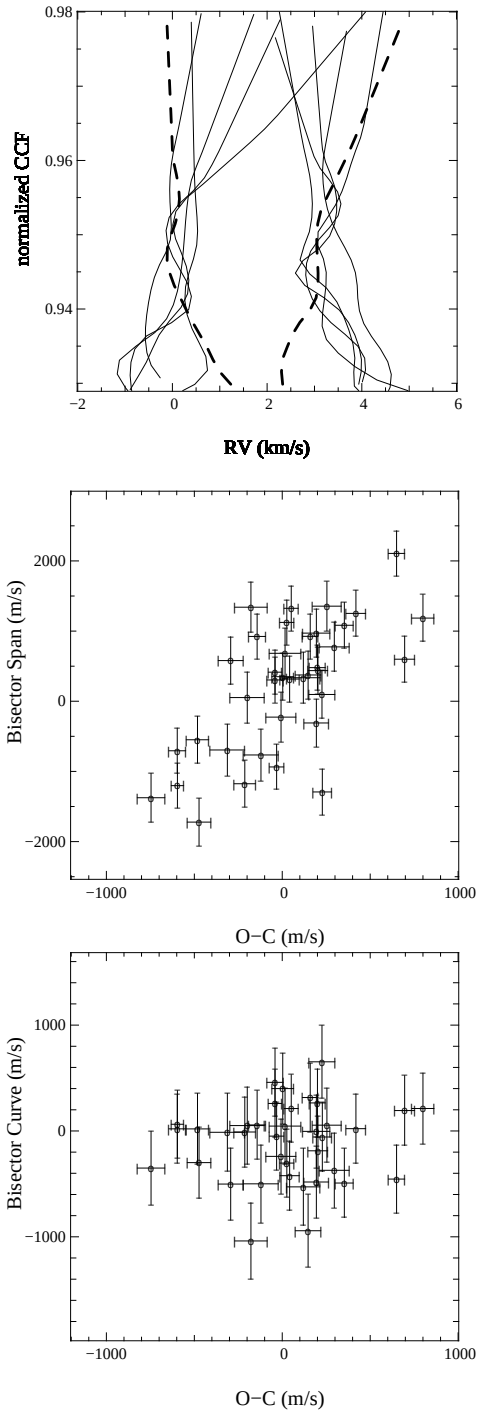

Fig. 6. Top: bisectors of the cross-correlation functions of HD 180777; only the bisectors of the spectra giving the largest residuals are represented, in 2 sets. Those corresponding to large positive (resp. negative) residuals have been translated to the left (resp. right), in order to better see the difference between them. Dashed lines represent the median bisectors of the dual set. Center: span of the bisectors as a function of the radial velocity residuals. Bottom: curvatures of the bisectors as a function of the residuals.

by the Moon, is very different from the one of HD 180777; cut frequencies applied during the radial velocity computation (Paper I) thus eliminate a potential contamination of the spectra.

Still, to rule out any possibility of artifact linked with the Moon's orbital motion, we show the radial velocities of a similar star in Fig. 5 , close to HD 180777 (declination of +55 degrees), but constant within the present level of uncertainties: HD 6961 is an A7V star with $v \sin i = 91\,\mathrm{km\,s^{-1}}$. It also belongs to our ELODIE sample. By July 2005, 15 spectra were gathered for this star, with an S/N equal to 266 on average. The typical uncertainty is $83\,\mathrm{m\,s^{-1}}$, comparable to the one obtained for HD 180777. The observed radial velocity dispersion of 63 $\mathrm{m\,s^{-1}}$ shows that this star is constant over the 440 days of the measurements (Fig. 5).

6. Radial-velocity residuals: pulsations

Considering the cross-correlation functions again, we can investigate whether the large radial-velocity residuals observed around the orbital solution can be related to the changes in the shape of these mean line profiles. We then compute the bisector of the cross-correlation functions (Fig. 6, top). A first step consists in calculating their span (or inverse slope), and to look for a correlation between the spans and the radial-velocity residuals. Figure 6 (center) shows the bisector spans as a function of these residuals: they seem to be linearly correlated, with a slope value close to 2. The changes in the shape of the lines thus appear to be responsible for at least a part of the radial-velocity residuals considered. Cool spots linked with magnetic activity are unlikely because in this case, the slope is negative (Queloz et al. 2001). Hot spots could be responsible for this correlation and cannot be excluded, although they are unlikely. Besides, the presence of a stellar binary system can produce this sort of linear correlation with a positive slope (Santos et al. 2002), but we checked (see Sect. 5) that it is not the case here, at least if the flux received from the two stars is similar. A remaining explanation is the presence of low order pulsations (Hatzes 1996).

As a second step, we calculated the curvature of the bisectors of the considered cross-correlation functions, as it is also shown to be useful for characterizing the pulsations (Hatzes 1996). The results are displayed on Fig. 6 (bottom) and do not show any correlation with the radial-velocity residuals. The bisectors thus mainly change with regard to their span; for a given variation of the span, we then expect around half this variation in the radial velocities (averaging effect). The slope value close to 2 found above between the bisector spans and the radial-velocity residuals then shows that the changes in the shape of the lines fully explain the dispersion of these residuals.

Even if our temporal sampling does not allow for a detailed analysis of short period variations, we are still able to enhance two frequencies characteristic of pulsations, at $1.324 \pm 0.001\,\mathrm{cycle\,d^{-1}}$ (period of 18.1 h) and $3.626 \pm 0.001\,\mathrm{cycle\,d^{-1}}$ (period of 6.6 h) (Fig 7, top). The false-alarm probabilities of these peaks are 0.34% and 8.4%, respectively, indicating a high significance for the $1.324\,\mathrm{cycle\,d^{-1}}$ signal, but a lower one for the $3.626\,\mathrm{cycle\,d^{-1}}$ signal. The phasing of the radial velocities to the corresponding periods is consistent with the existence of these signals (see Fig 7, bottom), as

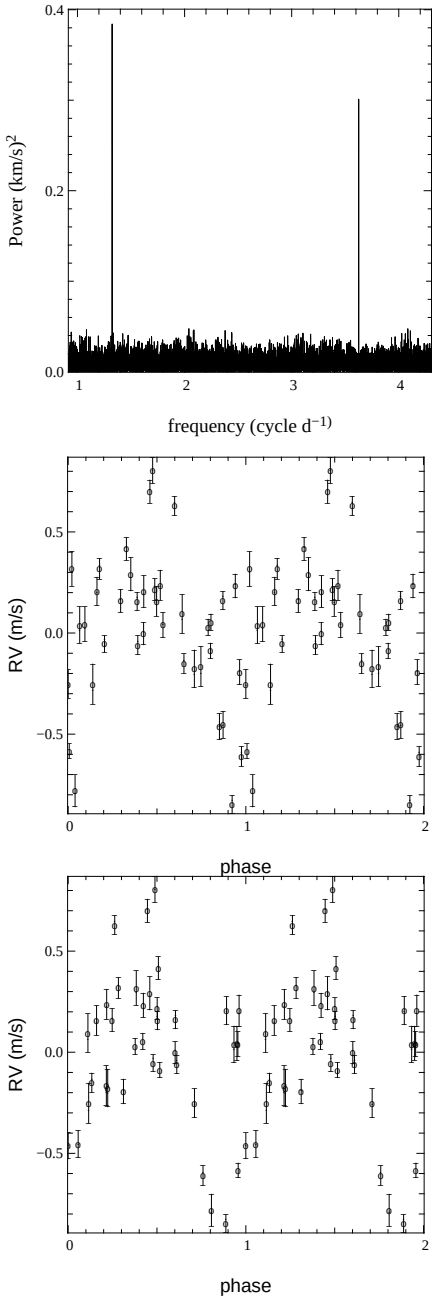

Fig. 7. High frequency periodograms of the radial velocities obtained on HD 180777 (top) and the phasing of the radial velocities to the corresponding periods (bottom).

well as the amplitudes of these radial-velocity variations (typically 200 m s^{-1}). A fit of the radial velocities with the superposition of two sinusoids with periods fixed to the above values leads to a decrease in the radial-velocity dispersion from 394 to 239 m s^{-1}, which is still well above the uncertainties (64 m s^{-1} on average). This convergence happens for values of the amplitude of 239 and 234 m s^{-1}, respectively. We are not able to detect other high frequencies, probably because of our temporal sampling, which is not really adapted to the search for high frequency variations.

The radial-velocity residuals observed around the orbital solution are thus very probably explained by changes in the shape of the lines created by pulsations of the star. The presence of pulsations in the case of HD 180777 is not surprising, as this star belongs to the range of B-V where the instability strip intersects with the main sequence, and where we find the pulsating δ Scuti (Handler et al. 2002, Breger et al. 2000) and γ Dor stars (Mathias et al. 2004, Handler et al. 2002). As the frequencies of the variations are lower than 0.25 cycle d^{-1} (periods larger than 6.5 h), HD 180777 should probably belong to the pulsating γ Dor stars. As these stars undergo non-radial pulsations resulting in multi-periodic radial-velocity variations with an amplitude up to several km s^{-1}, the level of 400 m s^{-1} found here for the radial-velocity residuals appears to be common.

We checked that the peak at 28.4 days is not an alias of these higher frequency signals. To do so, we first fitted the initial radial velocities with a double sinusoid with periods corresponding to the two high frequencies found above. The periodogram of the residuals obtained this way still shows a strong peak (with the same amplitude as in Fig. 1, bottom), at a frequency corresponding to the same period of 28.4 days. Hence, the signal at 28.4 days is not an alias of these high frequency signals.

7. Concluding remarks

We have presented here the first detection of a brown dwarf around one of the objects surveyed in our ELODIE programme, HD 180777, an A9V star with $v \sin i = 50$ km s^{-1}. This detection is an example of disentangling the presence of a low mass companion from the existence of pulsations. The best Keplerian solution derived from the radial-velocity measurements leads to a minimum mass of 25 M_{Jup} (the true mass could be significantly higher) and a period of 28.4 days, hence a separation of 0.2 AU.

It is interesting to note that the detected companion falls in the middle of the brown-dwarf desert observed for G-M dwarf primaries. For the first time, we are able to probe the mass-ratio of binaries with A-type dwarf primaries down to very small mass-ratios.

This result is another step toward extending the study of planet and brown-dwarf formation processes to stars earlier than F7. This is fundamental to a global understanding of the most interesting planetary formation mechanisms involved. In particular, the proposed idea that the planet formation process could scale with the primary mass is very interesting. Studies on lower mass stars (Ida & Lin 2005) show such a trend between the masses of the primaries and the companions. This idea is also consistent with the present detection of a brown dwarf around an A9V star. In such a picture, could brown dwarfs be formed in the same way as planets ?

Acknowledgements. We acknowledge support from the French CNRS. We are grateful to the Observatoire de Haute-Provence (OHP) and to the Programme National de Planétologie (PNP, INSU), for the time allocation, and to their technical staff. These results have made use of the SIMBAD database, operated at CDS, Strasbourg, France.

References

Baranne, A., Queloz, D., Mayor, M., et al. 1996, A&A 119, 373
Breger, M., Montgomery, M.H., 2000, ASP Conf. Ser., Vol. 210, Delta Scuti an Related stars. Astron. Soc. Pac., San Francisco
Chelli, A., 2000, A&A 358, L59
Galland, F., Lagrange, A.M., Udry, S., et al. 2005a, A&A, 443, 337
Galland, F., Lagrange, A.M., Udry, S., et al. 2005b, A&A, 444, L21
Galland, F., Lagrange, A.M., Udry, S., et al. 2006a, A&A, 447, 355
Gray, D., in *The Observation and Analysis of Stellar Photospheres*, Cambridge University Press, 2005
Handler, G., Balona, L.A., Shobbrook, R.R. et al. 2002, MNRAS 333, 262
Hatzes, 1996, PASP, 108, 839H
ESA 1997, The Hipparcos and Tycho Cat, ESA SP-1200
Hoffleit, D., Warren Jr, W.H., 1991, Bright Star Catalogue (5th Revised Ed.), NSSDC/ADC
Ida, S., Lin, D.N.C, 2005, ApJ, 626, 1045I
King, 2003, AJ, 125
Linnell Nemec, A. F., Nemec, J. M., 1985, BAAS, 17, 597
Marcy, G., et al. 2003, in *Scientific Frontiers in Research on Extrasolar Planets*, ASP Conf. Ser., in press
Mathias, P., Le Contel, J.-M., Chapellier, E., 2004, A&A, 417, 189
Pepe, F., Mayor, M., Rupprecht, G., et al. 2002, The ESO Messenger, 110, 9
Queloz, D., Henry, G. W., Sivan, J. P., et al., 2001, A&A, 379, 279
Roberts, D. H., Lehar, J., Dreher, J. W., 1987, AJ, 93, 968R
Santos, N.C., Mayor, M., Naef, D., et al. 2002, A&A, 392, 215